J Mater Sci: Mater Med (2010) 21:1421–1426
DOI 10.1007/s10856-010-4002-z

Electrochemical behaviour of Ti–Ni SMA and Co–Cr alloys in dynamic Tyrode's simulated body fluid

Chenghao Liang · Runfen Zheng · Naibao Huang · Bo Wu

Received: 24 August 2009 / Accepted: 10 January 2010 / Published online: 9 February 2010

Abstract The electrochemical behaviour of Ti–Ni shape memory alloy and Co–Cr alloys were investigated in dynamic Tyrode's simulated body fluid on a Model CP6 Potentiostat/Galvanostat. The results indicated that, for all alloys, the anodic dissolution and the pitting sensitivity increased with the flow rate of the Tyrode's solution increasing while the open-circuit potentials and pitting corrosion potentials decreased with the Tyrode's solution increasing. Pitting corrosion of Ti–Ni alloy was easier than Co–Cr alloys. Since the solution's flow enhanced oxygen transform and made it easy to reach the surface of electrodes, the plateau of oxygen diffusion control was diminished. All these indicated that the cathodic reduction and the corrosion reaction, which was controlled by the electrochemical mass transport process, were all accelerated in dynamic Tyrode's simulated body fluid.

1 Introduction

Ti–Ni shape memory alloy (abbreviated as Ti–Ni SMA) and Co–Cr alloys have already been used as biomaterials for a long time. Nowadays, they are applied in artificial joint, splint for fractured bone and artificial heart valve, etc. However, in the special environment of human body, the failures of implantation materials, caused by alloys' corrosion, are often encountered, which results in releasing metal ions and serious physiological reaction. As it is difficult to carry out corrosion tests in vivo, the experiments are commonly conducted in simulated body fluid. Some researchers have reported the corrosion resistance of Ti–Ni alloy and Co–Cr alloys in simulated body fluid [1, 2], which were performed in static condition, and the results could not reflect the actual corrosion process in the body correctly [3]. Hence, it is necessary to investigate the alloy's dynamic corrosion process.

In this paper, the dynamic cycle device, which was used to simulate the flowing of body fluid, was established and the electrochemical behaviours of Ti–Ni alloy and Co–Cr alloys were investigated at different flow rates in Tyrode's simulated body solution.

2 Materials and methods

2.1 Materials and solution

The tested materials, which were 10 × 10 × 2 mm, were Ti–Ni SMA and two kinds of Co–Cr alloys. The compositions of Ti–Ni SMA are Ti 50.8% (atomic proportion) and Ni 49.2%. The phase transition temperatures of Ti–Ni SMA were $A_s = 27°C$, $A_f = 56°C$. The Co–Cr alloys' compositions were showed in Table 1. The specimens were polished with abrasive paper (grade 360, 600, and 1000), and then, rinsed with distilled water, degreased with ethanol, and dried by air. 1 cm^2 was used as working area, and the residual area was covered by silicone resin. The tested solution was Tyrode's solution with components as follows: NaCl 8.00 g + KCl 0.20 g + $CaCl_2$ 0.20 g + $NaHCO_3$ 1.00 g + $MgCl_2$ 0.10 g + NaH_2PO_4 0.05 g + H_2O 1 l [4]. The solution's pH value was adjusted to 7.4 using 1 mol/l NaOH solutions.

C. Liang · N. Huang
Department of Materials Science and Engineering, Dalian Maritime University, Dalian 116026, China

C. Liang (✉) · R. Zheng · B. Wu
School of Chemical Engineering, Dalian University of Technology, Dalian 116012, People's Republic of China
e-mail: liangch@dlmu.edu.cn; lchenghao@126.com; liangch@chem.dlut.edu.cn

Table 1 Chemical composition of cobalt-based alloy (wt%)

Alloy	Mo	Cr	Fe	W	C	Si	Mn	Ni	Co
CoCrNiMo	5.0	25.0	3.1	2.1	0.06	0.38	0.7	8.9	Bal.
CoCrNiW	–	19.9	2.4	14.6	0.07	0.16	1.52	10.7	Bal.

2.2 Dynamic cycle device and electrochemical tests

The electrochemical tests were carried out in the dynamic cycle device (shown in Fig. 1), with flow rates 18.84 kg/h and 38.83 kg/h, respectively. The latter was the arterial blood's flow rate. According to the proportion of the gas in arterial blood, N_2, CO_2 and O_2 were aerated into the solution. The composition of the gas in arterial blood was shown in Table 2 [5]. In the process of aeration, the equipment was sealed with liquid. The gas in the solution arrived at a stable state after aerating for 30 min. Then the polarization tests were performed.

The electrochemical experiment was performed on a traditional three-electrode system with a platinum wire as counter-electrode and Ag/AgCl electrode as reference electrode. The test was carried out from the open circuit potential to the positive direction using a Model CP6 Potentiostat/Galvanostat (Made by Dalian University of Technology) with a scan rate of 0.5 mV s^{-1}. When the current density reached 1 mA/cm^2, reversal sweep was conducted. During anodic polarization, the potential at which the current density enlarged suddenly was defined as pitting potential. The potential at which the forward and backward polarization curves intersected was considered as protective potential Ep. The temperature of the solution was maintained at (37 ± 1)°C.

2.3 Corrosion rate test

After immersion for 48 h in the dynamic cycle device, the linear polarization was performed on a Model CP6 Potentiostat/Galvanostat. The polarization began from corrosion potential with a potential step of 0.5 nV, and the range of polarization potential was 20 mV. The slope of the linear polarization curves, R_p, was computed by least squares techniques [6], and then the alloys' corrosion rates were calculated. After polarization, scanning electron microscope (SEM, model PHILIPSXL-30) was used to observe the morphology of the sample.

Table 2 Gas concentration in Tyrode's solution and blood

Gas	Blood (mmHg)	Tyrode's solution (Vol%)
O_2	94.2	13.2
CO_2	37.8	5.4
N_2	571.7	81.4
H_2O	47.0	–
Total	750.7	100.0

3 Results

Fig. 2 showed the curves of corrosion potential vs. time for the alloys in Tyrode's solution with flow rates of 18.84 kg/h and 38.83 kg/h. They contain curves for Ti–Ni alloy (a), for Co–Cr–Ni–W alloy (b) and for Co–Cr–Ni–Mo alloy(c). From the curves, we knew that the corrosion potentials increased rapidly at first and then reached stable values after 500 min. In dynamic condition, the alloys' corrosion potential moved to negative direction (compared with the values in static solution). The bigger the flow rate was the more negative the alloys' corrosion potentials were. When the flow rate was 18.84 kg/h, the according corrosion potentials for Ti–Ni, Co–Cr–Ni–W and Co–Cr–Ni–Mo alloy were 45, 35 and 14 mV, respectively. While the flow rate increased to 38.83 kg/h, the according potentials were 115, 63 and 39 mV, respectively. Solution flowing accelerated the transfer Cl^- and OH^- and the dissolution of the

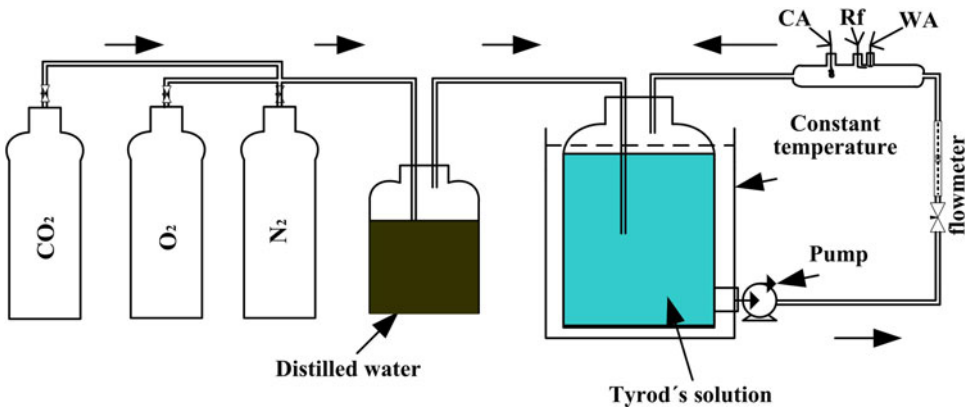

Fig. 1 Experimental instrument of flowing system

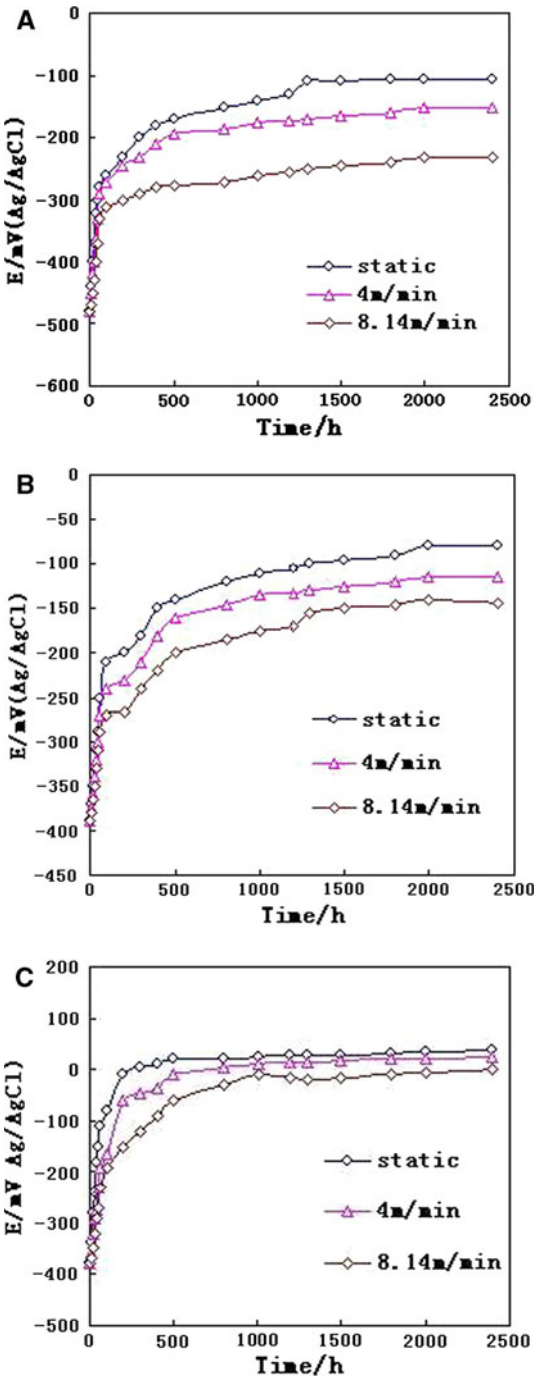

Fig. 2 Corrosion potential versus time curves of alloys in Tyrode's solution With different flow rates at 37°C. **a** TiNi SMA, **b** CoCrNiW alloy, **c** CoCrNiMo alloy

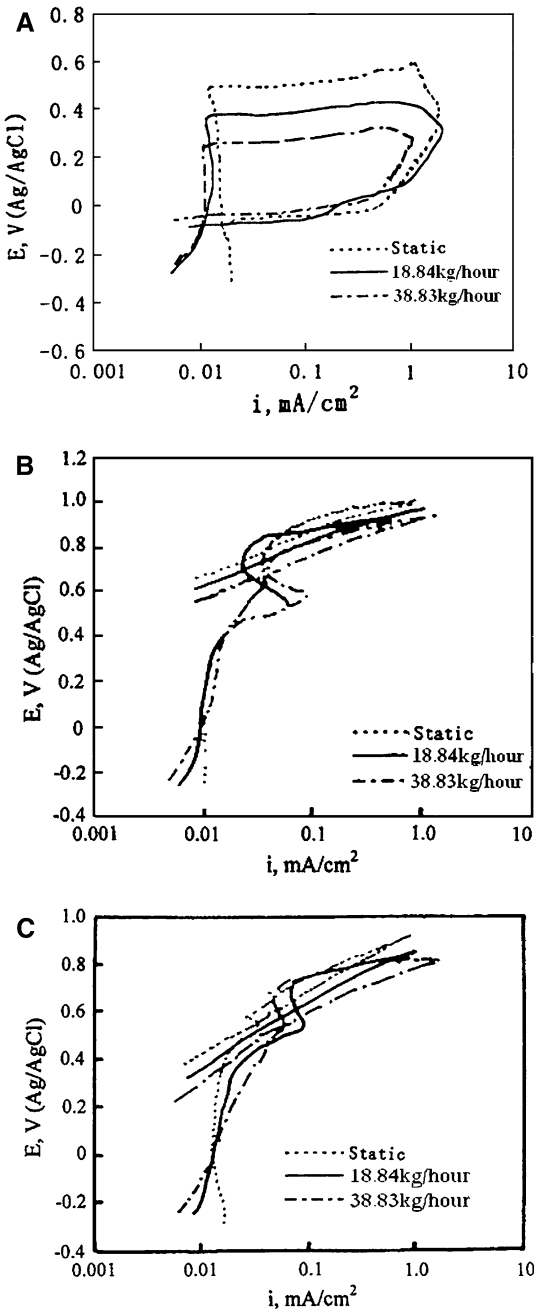

Fig. 3 Cyclic potentiodynamic polarization of alloys in Tyrode's solution With different flow rates at 37°C. **a** TiNi SMA, **b** CoCrNiW alloy, **c** CoCrNiMo alloy

alloy's passive film. Furthermore, it hastened the convective-diffusion, which leaded to the change of stress and inflected shearing stress. By all appearances, the flow of the medium made the alloy's electrochemical stability worsen and the alloy's corrosion potential moved to the negative direction.

The results of the cyclic polarization tests in Tyrode's solution with different flow rates at 37°C were shown in Fig. 3. For Ti–Ni alloy, a clear, wide and long hysteresis loop appeared (Fig. 3a). With the flow rate increasing, anodic current densities increased and breakdown potential E_b reduced, while its effect on protective potential E_p was little. SEM results indicated that visible pits appeared on Ti–Ni alloy surface after the tests were finished (Fig. 4a). These manifested that the increase of the flow rate

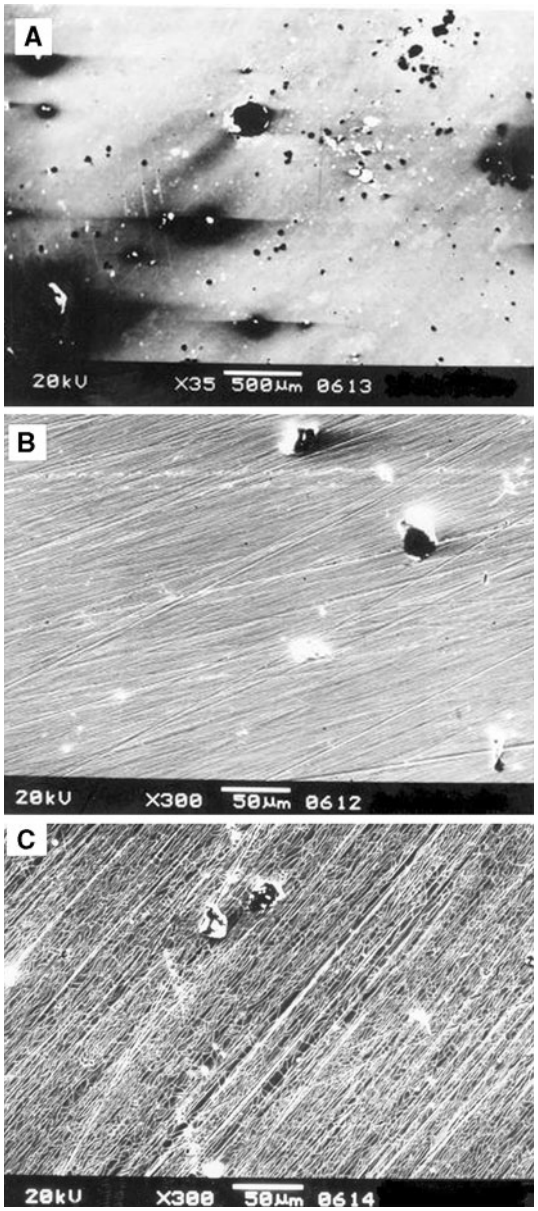

Fig. 4 SEM for alloys after immersed in dynamic Tyrode's solution. **a** TiNi SMA, **b** CoCrNiW alloy, **c** CoCrNiMo alloy

augmented the pitting corrosion sensitivity of Ti–Ni alloy. Whereas, Co–Cr alloys had small and narrow hysteresis loops, the influence of flow rate on E_b was not obvious. Only mini-pits appeared on the surface of alloys after test (Fig. 4b, c).

Table 3 showed the alloy's E_b values in Tyrode's solution with different flow rates. Aong them, E_b of Co–Cr–Ni–Mo was the most positive one. It indicated that this alloy had the best pitting corrosion resistance.

The alloys' cathodic polarization curves in Tyrode's solution were shown in Fig. 5. Along with the increase of flow rates, the plats of oxygen diffusion control were

Table 3 E_b of the alloys in Tyrode's solution with different flow rates (mV)

Alloy	Static solution	18.84 kg/h	38.83 kg/h
Ti–Ni	492	380	267
CoCrNiW	750	724	693
CoCrNiMo	782	753	728

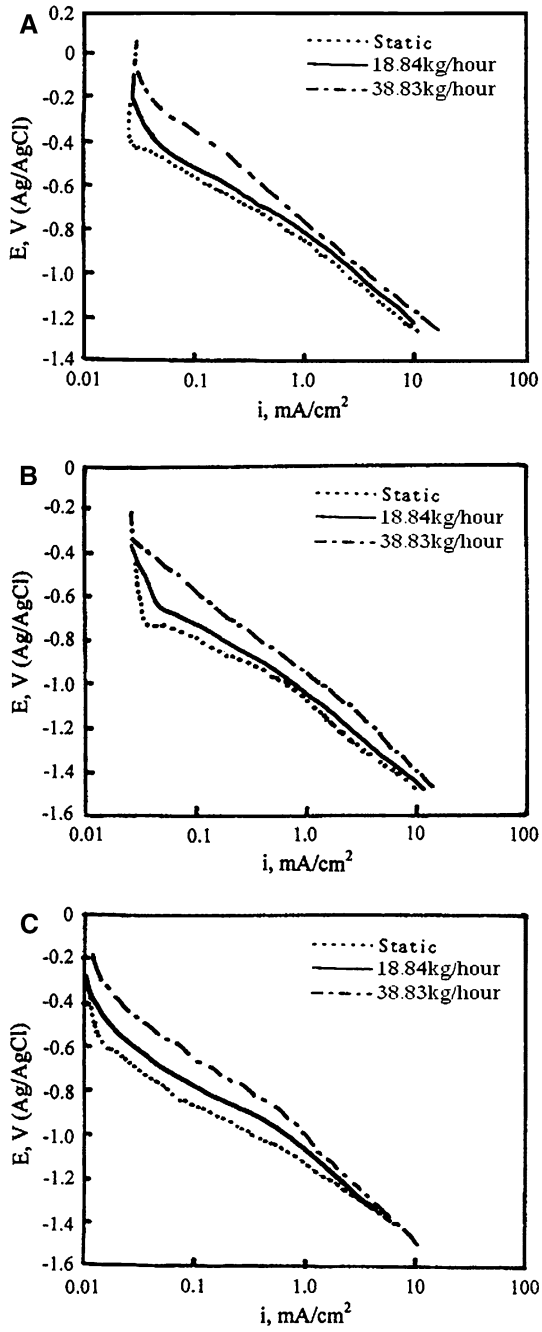

Fig. 5 Cathodic polarization curves of CoCrNiMo alloys in Tyrode's solution With different flow rates at 37°C. **a** TiNi SMA, **b** CoCrNiW alloy, **c** CoCrNiMo alloy

Table 4 The influence of flow rate on cathodic current densities at −600mv in Tyrode's solution (mA/cm^2)

Alloy	Static solution	18.84 kg/h	38.83 kg/h
Ti–Ni	0.101	0.204	0.412
CoCrNiW	0.029	0.041	0.105
CoCrNiMo	0.015	0.028	0.078

Table 5 Corrosion rates of alloys by transient linear polarization in Tyrode's solution

Alloy	Flow rates	R_p (MΩ·cm^2)	I (nA/cm$^{2)}$	Corrosion rate (μm/a)
Ti–Ni	Static	4.3812	4.5650	0.0691
	18.84 kg/h	9.9100	10.3258	0.1563
	38.83 kg/h	15.1348	15.7694	0.2387
CoCrNiW	Static	4.8180	4.1511	0.0490
	18.84 kg/h	10.5406	9.0816	0.1072
	38.83 kg/h	15.9879	13.7749	0.1626
CoCrNiMo	Static	5.7333	3.4884	0.0383
	18.84 kg/h	12.3648	7.5233	0.0826
	38.83 kg/h	18.5921	11.3123	0.1242

diminished. These indicated that solution flowing enhanced the transfer of oxygen, which resulted that electrochemical mass transport process became the control step of the corrosion reaction. Simultaneously, at the same potential, the polarization current densities increased with flow rate increasing. For instance, when the polarization potential was −600 mV (Table 4), the current density in dynamic condition was more than four times that in static condition. It was obvious that the flowage accelerated the cathodic reduction. However, when the polarization potential moved to a more negative value (<−1.2 V) and the evolution of hydrogen occurred, Whether the current density of cathodic polarization we at static condition or at dynamic conditions didn't make much difference. It was because that the reaction of hydrogen ion was controlled by electrochemical progress and the flowage had little influence on it.

Table 5 shows the corrosion rates of the alloys in Tyrode's solution with different flow rates by linear polarization technology. The results also indicated that solution flowing accelerated the alloys' corrosion. The corrosion rates under the flow rate of 38.83 kg/h were more than three times that in static state.

4 Discussion

Under normal conditions, Ti–Ni, Co–Cr–Ni–Mo and Co–Cr–Ni–W alloys had compact layer, which was little affacted by electrochemical corrosion. When the solution passed though the alloy's surface, the passive layer would be destroyed partially or entirely, and lost its protection. The fresh surface exposed to the corrosive solution. Furthermore, flowage would also reduce the concentration of metal ions near the alloy's surface. So, the alloys' electrochemical corrosion was accelerated (Table 5).

The resistance for the alloy's erosion corrosion was controlled by the performance of the passive layers. Electrode reactions of Ti–Ni and Co–Cr alloy in dynamic Tyrode's solution were as follows.

$$Ti + 2H_2O \rightarrow TiO_2 + 4H^+ + 4e \quad (1)$$

$$2Co + 3H_2O \rightarrow Co_2O_3 + 6H^+ + 6e \quad (2)$$

$$TiO_2 + 2H_2O \rightarrow Ti^{4+} + 4OH^- \quad (3)$$

$$Co_2O_3 + 3H_2O \rightarrow Co^{3+} + 6OH^-. \quad (4)$$

The above equations were the formation and the dissolution of passive layer.

Cathodic reaction

$$O_2 + 2H_2O + 4e \rightarrow 4OH^-. \quad (5)$$

Athough Ti–Ni alloy and Co–Cr alloys exhibited good abilities against general corrosion in dynamic Tyrode's solution, their pitting corrosion resistance made a difference. The augment of the flow rate made the E_b of Ti–Ni alloy decline obviously. The reason was that TiO_2 layer on the Ti–Ni alloy's surface was very crisp and easily destroyed in flowing solution [7], which not only reinforced the acidity in partial but also inhibited the repair of the passive layer. So, pitting corrosion occurred. For Co–Cr–Ni–Mo and Co–Cr–Ni–W alloys, they had well corrosion resistance and the Cr, Mo (or W) elements in the alloys adulterated into Co_2O_3 film (formula 2). All these improved the electrochemical stability of the layer and inhibited the erosion corrosion effectively.

5 Conclusions

(1) In Tyrode's solution, solution flowing decreased E_b of Ti–Ni and Co–Cr–Ni–W, Co–Cr–Ni–Mo alloys and accelerated their anodic dissolution. When the flow rate was 38.83 kg/h, the corresponding corrosion rate for the above mentioned alloys were 0.412 μm/a, 0.105 μm/a and 0.078 μm/a, respectively. Ti–Ni alloy's corrosion rate was bigger than that of Co–Cr alloys'.

(2) The cyclic potentiodynamic polarization showed the alloys' pitting corrosion sensitivity increased with the flow rate increasing. For Ti–Ni alloy, pitting corrosion easily occurred, while Co–Cr alloys had better pitting corrosion resistance.

(3) Since solution flowing enhanced the transform of oxygen, it influenced the alloys' cathodic polarization behaviors significantly. Under dynamic condition, the plats of oxygen diffusion control were inconspicuous and the electrochemical mass transport process became the control step.

Acknowledgements The author wishes to express her most sincere appreciation to Prof. H. Wang, who gave valuable advice during the experiments. Tremendous thanks were owed to Dr. W. Chen for the figures analysis.

References

1. Rondelli G, Vicentini B, Cigada A. The corrosion behaviour of nickel titanium shape memory alloys. Corros Sci. 1990;30:805–19.
2. Chenghao L, Haixia G. The effect of fibrinogen on the electrochemical behaviour of cobalt alloys in PBS solution. Chin J Biomed Eng. 2003;12:59–65.
3. Duan Y, Liu K, Chen J. Effect of simulated body fluid flowing rate on bone-like apatite formation on porus calcium phosphate ceramics. Space Med Med Eng. 2002;15:203–7. (in Chinese).
4. Chenghhao L, Liang G, Wan C, et al. Electrochemical behavior of SUS316L stainless steel after surface modification. Trans Nonferrous Metals Soc China. 2003;13:398–401.
5. Pu S. Metallic implant materials and corrosion. Beijing: Beijing University of Aviation and Space flight; 1990. p. 62–6.
6. Jones DA. Electrochemical measurement of low corrosion rate. Corros NACE. 1966;22:198–205.
7. Kazuhiko E. Corrosion resistance of Ni-containing alloys. In: Corrosion and protection 126th conference. Tokyo; 1999. p. 36–45.